Adsorption Characteristics of Lead-, Barium- and Hydrogen-rich Clinoptilolite Mineral

Fehime Cakicioglu-Ozkan* and Semra Ulku *Chemical Engineering Department, Engineering Faculty, Izmir Institute of Technology, Gulbahce Koyu, 35437 Urla, Izmir, Turkey.*

(Received 3 December 2002; revised form accepted 26 February 2003)

ABSTRACT: The carbon dioxide and water vapour adsorption properties of local clinoptilolite-rich material, both as the original and as lead-, barium- and hydrogen-rich forms, were examined. The lead- and barium-rich forms were prepared by treatment of the original clinoptilolite with $Pb(NO_3)_2$ and $BaCl_2$ respectively, while the hydrogen-rich form was prepared by NH_4Cl and heat treatment. Water and CO_2 adsorption experiments were conducted in a volumetric system under static conditions, with low-pressure adsorption data being used for the characterization of the natural, Pb-rich, Ba-rich and H-rich clinoptilolite samples. Although the existence of barium-exchange was not noted, an appreciable decrease in CO_2 adsorption was observed with the Pb-rich and H-rich forms due to a decrease in the electrostatic interaction between the surface and the adsorbate. Application of the Dubinin–Astakhov equation to the water adsorption data established the existence of micropores of different sizes that exhibited different adsorption mechanisms.

INTRODUCTION

Clinoptilolite is one of the most common natural zeolite minerals with a wide range of application. A comprehensive review relating to its large-scale application has been published by Ackley *et al.* (1992). The basic structure of the clinoptilolite crystal contains three types of channels with the following approximate dimensions: channel A (7.2 Å × 4.4 Å); channel B (4.0 Å × 5.5 Å); and channel C (4.1 Å × 4.0 Å). Channels A and B, which are parallel to each other, are intersected by channel C and exchangeable charge-balancing cations (Ca^{2+}, Mg^{2+}, Na^+, K^+, etc.) are located in these channels. Thus, channel A is occupied by calcium, magnesium and (preferentially) sodium ions; channel B is occupied by sodium and (preferentially) calcium ions; while channel C is occupied by potassium ions. All these cations are coordinated with the framework oxygen atoms and/or water molecules (Ackley *et al.* 1992).

Clinoptilolite-rich mineral, which is composed of clinoptilolite crystals and impurities functioning as binding agents, has a polydisperse pore-size distribution. The purity of the mineral and the location and type of cations, which effect the pore and channel dimensions, change from one deposit to another. All these factors influence the adsorption properties of the material significantly and for this reason clinoptilolite and its ion-exchange derivatives offer versatility for selective separation. Although the adsorption characteristics of clinoptilolite from different origins have been studied extensively (Arcoya *et al.* 1994; Tsitsishvili *et al.* 1992), commercial application has been limited due to the changes in the properties from one deposit to other. The characterization of clinoptilolite is the most important step in ensuring the application of this mineral as an adsorbent.

*Author to whom all correspondence should be addressed. E-mail: fehimeozkan@iyte.edu.tr.

Clinoptilolitehas a special value, especially for the adsorption of small size molecules such as CO, H_2O, CO_2, NO and NH_3. Adsorption studies of these molecules provide information on the properties of the adsorbent (pore volume, pore size, specific surface area, adsorption energetics) and also the potential value of the mineral for industrial application. In the present study, the pore structure of the local Turkish (Bigadiç) clinoptilolite-rich mineral has been changed and the adsorption properties of the original and modified forms towards water vapour and carbon dioxide investigated.

EXPERIMENTAL

Materials

Clinoptilolite-rich mineral from Bigadiç, Turkey, as identified previously, was used in its original and modified forms. The original mineral was crushed, ground and washed with doubly distilled water to remove soluble impurities and analyzed using wet chemical methods and X-ray diffraction. A Varian 10BQ atomic absorption spectrophotometer was used in the wet chemical analysis of the mineral, while the X-ray diffraction spectrum of the mineral was obtained using a Philips PW 1840 diffractometer in conjunction with Cu Kα radiation and an Ni filter.

The washed samples, which were dried in a vacuum oven at 160°C for 24 h, were used in cation-exchange and adsorption studies.

Methods

Modification of original material by cation exchange

Since the type, location and concentration of the cations were expected to play an important part in the adsorption properties of the clinoptilolites, various cations (Ba^{2+}, Pb^{2+}, NH_4^+) were incorporated into the structure of the local zeolite to generate Ba-rich, Pb-rich and H-rich zeolites. For such cation-exchange experiments, the following exchange solution concentrations were employed:

$BaCl_2$: 0.001 M; 0.005 M; 0.01 M; 0.03 M; 0.05 M; 0.1 M.

$Pb(NO_3)_2$: 0.001 M; 0.005 M; 0.01 M; 0.05 M; 0.1 M.

The experiments employed 5 g of washed zeolite treated at 25°C for 3 d with 100 ml of an exchange solution of known concentration, the exchange solution being renewed at 24-h intervals. The exchange solution samples were separated by filtration and analyzed by atomic absorption spectrophotometry to determine the amounts of Na, K, Mg, Ca, Ba and Pb cations exchanged. The treated samples were then washed with distilled water until no Cl^- or NO_3^- anions were detected in the wash water, following which they were stored for subsequent adsorption experiments.

For the preparation of the Pb-rich form, use was made of the NH_4^+-rich form of the zeolite as prepared from the original zeolite rather than the original mineral. The NH_4^+-rich form was obtained on treating the washed samples with 1.5 M NH_4Cl for 3 d at 25°C. This form was converted to the hydrogen-rich form by heating in an oven at 400°C.

Volumetric adsorption system

An OMNISORP 100CX volumetric adsorption system fitted with adsorption and outgassing ports was used for adsorption experiments. For each adsorption run, optimum outgassing conditions

were determined by performing adsorption experiments under different outgassing temperatures, pressures and times. The optimum outgassing conditions thus established for the zeolite were 16 h, 400°C and 10^{-6} mbar pressure. These were used in all subsequent adsorption experiments.

Adsorption data for water vapour (Özkan 1996) and carbon dioxide (Demirci 1996) were collected using the static method in which a known quantity of the pure adsorbate (i.e. 30 Torr for CO_2 adsorption and 20 Torr for H_2O vapour adsorption) was admitted into a confined volume containing the adsorbent sample at 25°C. The pressure in the confined volume, which decreased as adsorption proceeded to equilibrium, was followed (equilibration sampling time: 10 s; number of equilibration sample points: 18) and the equilibrium values recorded. The corresponding adsorption isotherms were constructed point-by-point by the admission of successive charges of CO_2 or H_2O vapour.

RESULTS AND DISCUSSION

The chemical composition of the clinoptilolite-rich mineral (wt%) was SiO_2, 71.75; Al_2O_3, 10.91; Fe_2O_3, 0.54; MgO, 1.08; CaO, 2.3; Na_2O, 1.19; K_2O, 4.3; TiO_2, 0.17; MnO_2, 0.0008; and H_2O, 7.77. The X-ray diffraction diagram depicted in Figure 1 exhibited characteristic clinoptilolite peaks (Gottardi and Galli 1985) at $2\theta = 9.87°$, 22.4° and 30°, respectively.

Cation exchange

The exchange degree, X_i, for each cation, i:

$$X_i = \frac{(C_{i,o} - C_{i,f})}{C_{i,o}} \times 100 \quad (1)$$

where $C_{i,o}$ and $C_{i,f}$ are the initial and the final cation concentrations in the clinoptilolite-rich zeolite at the end of the exchange, was determined using chemical analysis of the exchange solutions. The quantities of Ba^{2+} and Pb^{2+} ions exchanged (mequiv Ba^{2+}/100 g zeolite and mequiv Pb^{2+}/100 g zeolite) as a function of the initial solution concentration, calculated from the total amount of cation (Ca^{2+}, Mg^{2+}, K^+, Na^+) removed from the clinoptilolite-rich zeolite mineral, are presented in Figures 2(a) and (b).

For $BaCl_2$, the total amount of cation exchanged (mequiv Ba^{2+}/100 g zeolite) increased on increasing the $BaCl_2$ concentration up to 0.01 M. However, at increasing concentrations in the

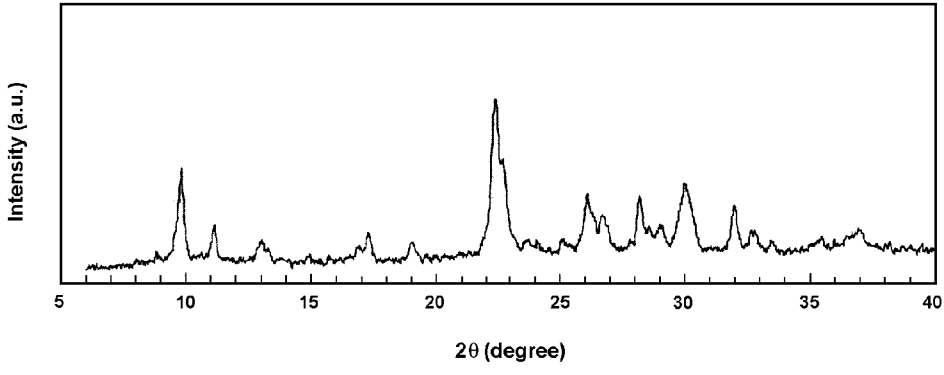

Figure 1. X-Ray diffraction pattern of original zeolite mineral from Bigadiç, Turkey.

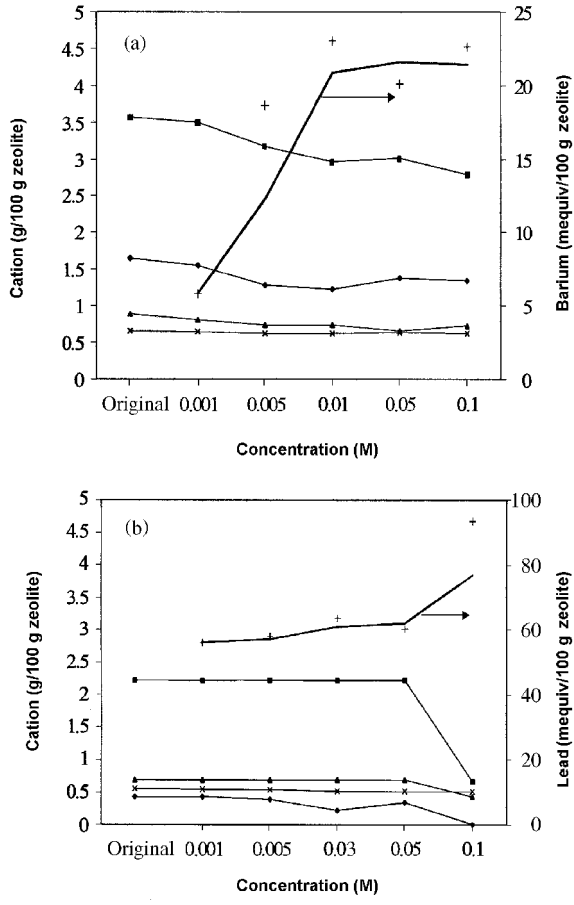

Figure 2. Cation content of (a) Ba-rich zeolites and (b) Pb-rich zeolites. Symbols: ■, K^+; ▲, Na^+; ✕, Mg^{2+}; ◆, Ca^{2+}; +, Ba^{2+} or Pb^{2+}.

range 0.01–0.1 M, the exchange was not significantly affected by the concentration [Figure 2(a)]. Thus, the X_K, X_{Na} and X_{Ca} values changed from 2%, 9% and 2% to 22%, 19% and 19% with increasing $BaCl_2$ solution concentration. However, the X_{Mg} values were quite low (ca. 5%) and were not affected significantly by the concentration.

In the case of Pb exchange, the total amount of cation exchanged (mequiv Pb^{2+}/100 g zeolite) increased only slightly with increasing concentration up to 0.05 M and reached a value of 93 mequiv/100 mg zeolite at the highest $BaCl_2$ concentration (0.1 M). As seen from Figure 2(b), the X_{Ca} value changed from 10% to 100% with increasing $Pb(NO_3)_2$ concentration while the value of X_{Mg} was hardly affected and remained low (ca. 5%). For univalent ions (K^+ and Na^+), almost no exchange occurred at low concentrations [≤ 0.05 M $Pb(NO_3)_2$] whereas the X_K and X_{Na} values were 55% and 37% at the highest $Pb(NO_3)_2$ concentration (0.1 M).

The radii of the hydrated cations (4.28 Å, 4.12 Å, 3.58 Å and 3.31 Å for Mg^{2+}, Ca^{2+}, Na^+ and K^+, respectively) and the location of cation sites seemed to be effective in the cation-exchange studies. Since the radius of the hydrated Mg^{2+} ion is greater than that of the others, Mg^{2+} ions cannot be removed readily from the structure. Thus, mainly Ca^{2+} ions (ionic radius, 0.99 Å) and

K^+ ions (ionic radius, 1.3 Å) were exchanged with the NH_4^+ and Ba^{2+} ions (ionic radii, 1.35 Å and 1.5 Å, respectively) during the cation-exchange studies.

Adsorption isotherms

The water vapour and carbon dioxide adsorption isotherms for the Ba-rich and Pb-rich forms are depicted in Figures 3(a) and (b), respectively. The water vapour adsorption isotherms [Figure 3(a)] demonstrate that the effect of barium exchange on water adsorption was not appreciable. In contrast, for CO_2 adsorption, a considerable decrease in the amount adsorbed occurred in the presence of the Pb-rich forms [Figure 3(b)]. The H-rich zeolite also gave a lower adsorption capacity relative to that of the original zeolite, whereas a similar behaviour was not observed for the Ba-rich forms.

This variation may be related to the electrostatic field created by the cation located in the zeolite pores. Substitution of ions of greater electronegativity such as H^+ and Pb^{2+} (Pauling electronegativity values of 1.9, 2.1 and 0.9 for H^+, Pb^{2+} and Ba^{2+}, respectively) causes a decrease in the electrostatic field strength at the surface. This leads to a decrease in the adsorption of carbon dioxide.

Adsorption characteristics

Values of the adsorption characteristics, i.e. the monolayer adsorption capacity (V_m), the apparent micropore volume (W_0), the specific surface area (A_m) and the Dubinin–Astakhov model (Dubinin

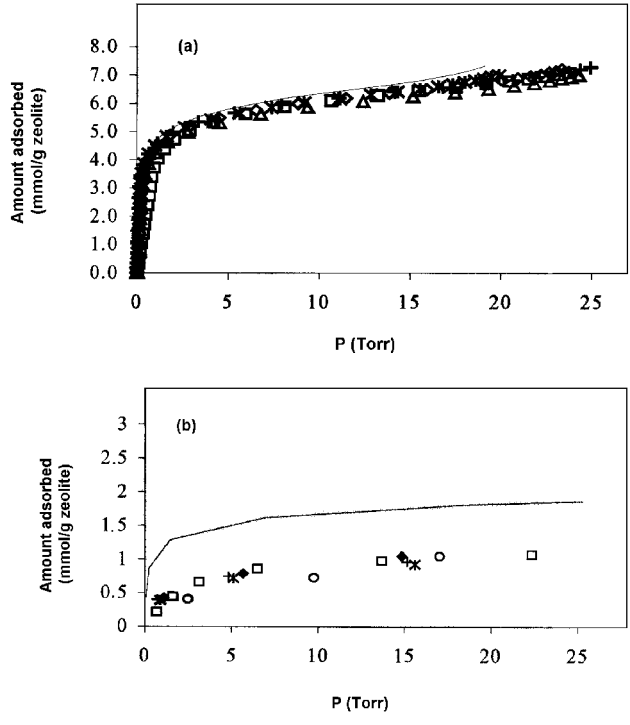

Figure 3. Isotherms for (a) water vapour sorption on Ba-rich zeolites and (b) carbon dioxide sorption on Pb-rich zeolites. Symbols: (a): —, Original; +, 0.001 M; □, 0.005 M; ◇, 0.01 M; ✱, 0.05 M; △, 0.1 M. (b): —, Original; ○, 0.001 M; ♦, 0.005 M; ✱, 0.03 M; +, 0.05 M; □, 0.1 M.

1960) parameters (E and n), for the natural and modified zeolites were calculated from the data obtained in the water vapour and carbon dioxide adsorption experiments. These are presented in Tables 1 and 2 for comparative purposes. The parameters E and n were determined for a specific adsorbent/adsorbate pair using the D–A plot [log W versus $\log(P^0/P)^n$] over the relative pressure range $0.06 < P/P^0 < 0.1$ and used to describe the energetic and structural heterogeneities of the

TABLE 1. Water Vapour Adsorption Characteristics of Original and Cation-exchanged Zeolites

Cation solutions	n	E (kJ/mol)	A_m (m^2/g)	V_m (cm^3/g)	W_0 (cm^3/g)	V_{max} (cm^3/g)
Original	2.5	10.4	383	0.109	0.103	0.129
0.001 M $BaCl_2$	2.4	15.1	383	0.109	0.102	0.136
0.005 M $BaCl_2$	2.1	12.7	383	0.109	0.125	0.132
0.010 M $BaCl_2$	2.6	14.4	383	0.109	0.101	0.126
0.050 M $BaCl_2$	2.7	14.2	376	0.107	0.098	0.129
0.100 M $BaCl_2$	2.5	13.9	373	0.109	0.101	0.125
0.001 M $Pb(NO_3)_2$	2.3	10.63	404	0.115	0.113	0.129
0.005 M $Pb(NO_3)_2$	2.4	11.03	417	0.119	0.117	0.136
0.010 M $Pb(NO_3)_2$	2.3	9.33	390	0.111	0.114	0.141
0.030 M $Pb(NO_3)_2$	2.3	11.21	375	0.107	0.100	0.130
0.050 M $Pb(NO_3)_2$	2.3	10.46	374	0.099	0.095	0.126
0.100 M $Pb(NO_3)_2$	2.6	10.55	388	0.111	0.103	0.115
1.500 M NH_4Cl	2.1	9.88	372	0.116	0.110	0.136

TABLE 2. Carbon Dioxide Adsorption Characteristics of Original and Cation-exchanged Zeolites

Cation solutions	n	E (kJ/mol)	A_m (m^2/g)	V_m (cm^3/g)	W_0 (cm^3/g)	V_{max} (cm^3/g)
Original	2.3	17.9	259	0.092	0.088	0.092
0.001 M $BaCl_2$	3.2	14.8	254	0.089	0.086	0.089
0.005 M $BaCl_2$	2.9	16.4	262	0.093	0.088	0.092
0.010 M $BaCl_2$	2.6	17.9	260	0.091	0.087	0.092
0.050 M $BaCl_2$	2.8	16.9	258	0.091	0.091	0.092
0.100 M $BaCl_2$	2.9	16.1	251	0.089	0.084	0.088
0.001 M $Pb(NO_3)_2$	1.9	12.4	254	0.090	0.104	0.104
0.005 M $Pb(NO_3)_2$	1.9	14.4	246	0.087	0.084	0.092
0.010 M $Pb(NO_3)_2$	1.9	13.9	234	0.083	0.083	0.092
0.030 M $Pb(NO_3)_2$	1.8	16.5	196	0.069	0.067	0.077
0.050 M $Pb(NO_3)_2$	1.7	16.6	203	0.072	0.074	0.082
0.100 M $Pb(NO_3)_2$	2.0	15.0	184	0.065	0.065	0.068
1.500 M NH_4Cl	1.9	11.9	240	0.069	0.069	0.075

samples (Chen and Yang 1996). The apparent micropore volume was obtained by extrapolating the linear portion of the Dubinin–Astakhov plot.

Representative Dubinin–Astakhov plots, which give a quantitative assessment of the microporosity of the sample (Bradley and Rand 1995), are given for water and carbon dioxide adsorption in Figures 4(a) and (b), respectively. Although the D–A plots for CO_2 adsorption were almost linear over the relative pressure range 10^{-3}–10^{-1}, a deviation from linearity which is frequently encountered was observed for the adsorption of water vapour, indicating heterogeneity in the micropore structure. This heterogeneity may be due to the presence of impurities in the zeolite structure.

The apparent micropore volumes,

$$W = \frac{V}{22\,400\rho^*} \tag{2}$$

were calculated using the corrected liquid density, ρ^*, at the adsorption temperature, T, as expressed by Dubinin (1960):

$$\rho^* = \rho_b - n(T - T_b) \tag{3}$$

where $n = (\rho_b - \rho_m)/(T_c - T_b)$ and $\rho_m = MW/b$, with ρ_m and ρ_b being the density of the adsorbate molecule at the critical temperature, T_c, and the boiling temperature, T_b, respectively, while MW

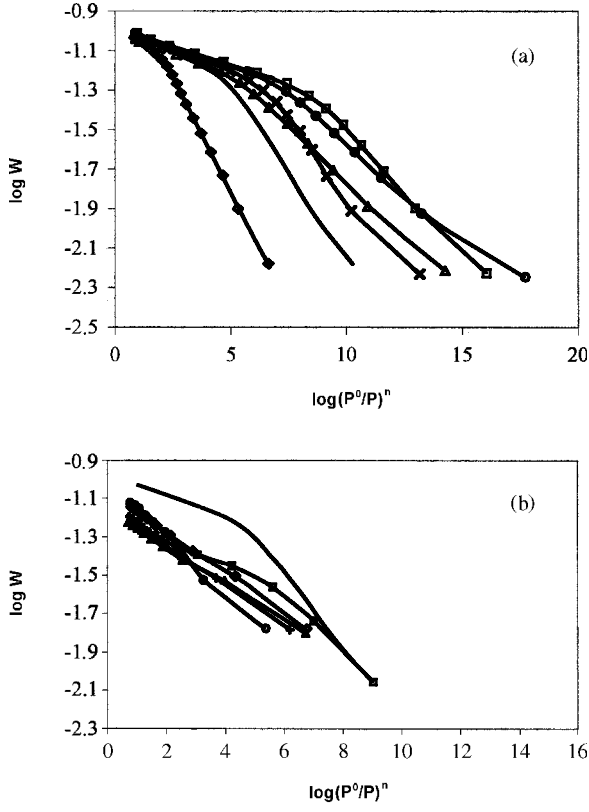

Figure 4. Dubinin–Astakhov plots for (a) water vapour sorption on Ba-rich zeolites and (b) carbon dioxide sorption on Pb-rich zeolites. Symbols: (a): —, Original; □, 0.001 M; ◇, 0.005 M; ○, 0.01 M; ×, 0.05 M; △, 0.1 M. (b): —, Original; ○, 0.001 M; ◇, 0.005 M; △, 0.03 M; +, 0.05 M; □, 0.1 M.

and b are the molecular weight and van der Waals constant, respectively. The area occupied by a single carbon dioxide molecule is equal to 18.4 $Å^2$ if use is made of the corrected density for carbon dioxide as proposed by Dubinin (1960), while the same quantity calculated using the bulk density is equal to 22.9 $Å^2$. This discrepancy could indicate that the effect of packing the linear CO_2 molecule (length, 5.1 Å; width, 3.7 Å; van der Waals diameter, 3.2 Å) on the zeolite surface may also be important. In fact, there is some debate as to which value of the density should be used in the calculations. In the present study, the value of 18.4 $Å^2$ has been used as the molecular area of CO_2.

As seen from Tables 1 and 2, the V_m values agreed well with the W_0 values, suggesting that the sorption of CO_2 and H_2O molecules in the micropores led to spontaneous filling of the micropore volume and the development of monolayer coverage. At $P/P^0 = 0.85$, the V_{max} values were higher than the V_m and W_0 values for water vapour sorption, whereas all three values were close to each other for carbon dioxide sorption suggesting an adsorption mechanism without multilayer formation. The high V_{max} values obtained from the water sorption data could be related to the existence of impurities or other zeolite phases in the zeolite sample studied.

The E parameter of the D–A equation obtained from the adsorption of either CO_2 or H_2O indicated that the characteristic adsorption energy obtained for the Ba-rich zeolites was generally higher than those for the Pb-rich and H-rich forms. It will be seen from the data recorded in Tables 1 and 2 that the values of E for these modified zeolites were higher for CO_2 adsorption relative to H_2O adsorption. This behaviour may be related to the strength of the interaction energy effected by the electric field, which depends upon the electronegativity of the cation and also the polarizability of the adsorbate [the polarizability of the CO_2 molecule (2.91×10^{-3} nm^3) is higher than that of the water molecule (1.4×10^{-3} nm^3)].

Tables 1 and 2 also show a comparison of the specific surface areas, A_m, of the zeolites as calculated from the CO_2 and H_2O adsorption data using the Langmuir equation. The specific surface areas obtained from the CO_2 data were lower than from the water vapour data for the zeolites. This difference may be related to the difference in the adsorption capacity, packing and interaction of CO_2 and H_2O molecules with ions on the surface, and also to the assumptions made for the adsorbate densities that are highly questionable especially for molecules whose shape differs from that of a sphere.

The cation-exchange processes involved in this study, i.e. Ba exchange and Pb exchange, proved very effective towards CO_2 adsorption. The high sensitivity of CO_2 molecules to the properties of the cations (electronegativity, ionic radius, charge) was the main factor influencing the adsorption properties of this compound. The adsorption behaviour of water vapour was virtually the same for the Pb-rich, Ba-rich and H-rich zeolite. However, the presence of different adsorption mechanisms and the structural heterogeneity of the zeolitic material were both very effective in water vapour sorption.

ACKNOWLEDGMENTS

The authors thank Professor Devrim Balköse for useful discussions and advice. They also wish to express their grateful appreciation to the Ege University Research Foundation for financial support.

REFERENCES

Ackley, M.W., Giese, R.F. and Yang, R.T. (1992) *Zeolites* **12,** 780.
Arcoya, A., Gonzales, J.A., Travieso, N. and Seoane, X.L. (1994) *Clay Miner.* **29,** 123.

Bradley, R.H. and Rand, B. (1995) *J. Colloid Interface Sci.* **169,** 168.
Chen, S.G. and Yang, R.T. (1996) *J. Colloid Interface Sci.* **177,** 298.
Demirci, A. (1996) *MS thesis,* Ege University, Turkey.
Dubinin, M.M. (1960) *Chem. Rev.* **60,** 235.
Gottardi, G. and Galli, E. (1985) *Natural Zeolites,* Springer-Verlag, Berlin.
Özkan, F. (1996) *PhD thesis,* Ege University, Turkey.
Tsitsishvili, G.V., Andronikashvili, T.G., Kirov, G.N. and Filizova, L.D. (1992) *Natural Zeolites,* Ellis Horwood, New York.